Transactions of the 17th International Conference on Structural Mechanics in Reactor Technology (SMiRT 17)
Prague, Czech Republic, August 17 –22, 2003
Paper # WG01-3

A Simulation of Corrosion Fatigue Crack Growth

Petr Brož [1)]

[1)] Czech Technical University

ABSTRACT

Based on a dislocation representation of short cracks, the Navarro-de los Rios simulation presents the productive essentials by means of to investigate the characteristics of micro-sensitive cracks. In the contribution proposed, the influence of the environment is put on the model by incorporating pit propagation kinetics, adapted (ie environment affected) crack growth equations and lifetime analyses. The model employed yields a forcible interpretation of the experimental evidence and offers a suitable predictive algorithm for fatigue crack propagation characteristics and eventual failure.

KEY WORDS: air, dissolution law, environment, incubation time, microstructural barriers, pit initiation.

INTRODUCTION

Fatigue cracks are invariably initiated at corrosion pits formed at inclusions, consequently the analysis includes stress concentration influences at pits that lead to the propagation of fatigue cracks the rates of which are considered to be proportional to the crack tip plastic displacement [1]. This plasticity is constrained by microstructural barriers that are conquer in a non-aggressive environment at critical crack lengths only when the applied stress is higher than the fatigue limit. But still, the superposition of an aggressive environment assists fatigue damage by means of crack tip dissolving enhancement of crack tip plastic deformation, the introduction of stress concentrations at dents and a reduction of the strength of the microstructural barrier. These environment effects are demonstrated in a radical reduction of the fatigue limit and higher crack propagation rates.

In the contribution presented, the influence of the environment is incorporated into the model by including pit growth kinetics, stress concentration at pits, environment affected crack propagation equations and lifetime analysis. The environment raises crack tip plasticity, namely increases crack growth rates and reduces the strength of the microstructural barriers that is demonstrated by reductions in fatigue resistance and the fatigue limit.

GENERALIZED CORROSION – FATIGUE CHARACTERISTICS

Corrosion-fatigue behaviour of a given environment-material system refers to the characteristics of the material under fluctuating loads in the presence of the particular environment. Different environments have various effects on the cyclic behaviour of a given material. Similarly, the corrosion-fatigue behaviour of different materials is different in the same environment [2].

The corrosion-fatigue behaviour of metals subjected to load fluctuation in the presence of an environment to which the metal is resistant, is identical to the fatigue behaviour of the metal in the absence of that environment. Consequently, the corrosion-fatigue behaviour of an environment-material system can be studied by setting up the variance of the corrosion-fatigue behaviour for the environment-material system from the fatigue behaviour of the material in a benign environment.

Stress-corrosion crack growth in a statically loaded structure is caused by interactions of chemical and mechanical processes at the crack tip. The highest plane-strain stress-intensity-factor value at which subcritical crack growth does not occur in a material loaded statically in an aggressive environment is designated K_{Iscc}. Consequently, to found the effect of an environment on the fatigue-crack-growth behaviour of a material, the fatigue-crack-growth behaviour for the material in a benign environment and the K_{Iscc} for the environment-material system should be established first as references.

The generalized fatigue-crack-growth behaviour in a benign environment (Fig. 1), is a special case of the corrosion-fatigue crack propagation characteristics for metals. It represents the „corrosion-fatigue“ behaviour of metals subjected to load fluctuations in the presence of any environment that does not affect the fatigue-crack-growth behaviour for the metal. Thus, the corrosion-fatigue behaviour for a given environment-material system could be investigated by establishing the base-line fatigue behaviour and then by determining the effect of the environment on the fatigue behaviour regions I, II, and III (Fig. 1). But still, because K_{Iscc} for an environment-material system defines the plane-strain K_I value above which stress-corrosion crack growth can occur under static loads, the corrosion-fatigue crack-propagation behaviour for the environment-material system could be altered when the maximum value of K_I, K_{Imax}, in a given load cycle becomes greater than K_{Iscc}. That is why the corrosion-fatigue crack-propagation behaviour should be separated into below – K_{Iscc} and above – K_{Iscc} behaviours.

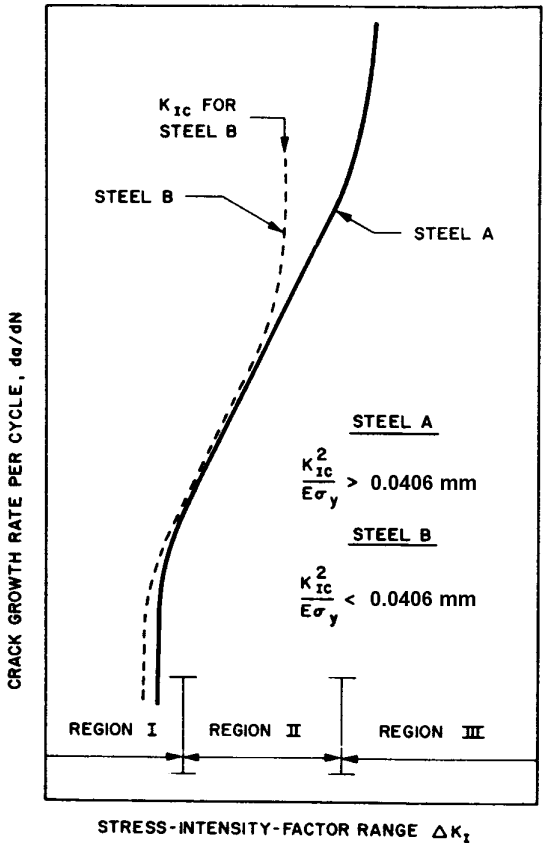

Fig. 1 Simplistic representation of fatigue-crack growth in steel

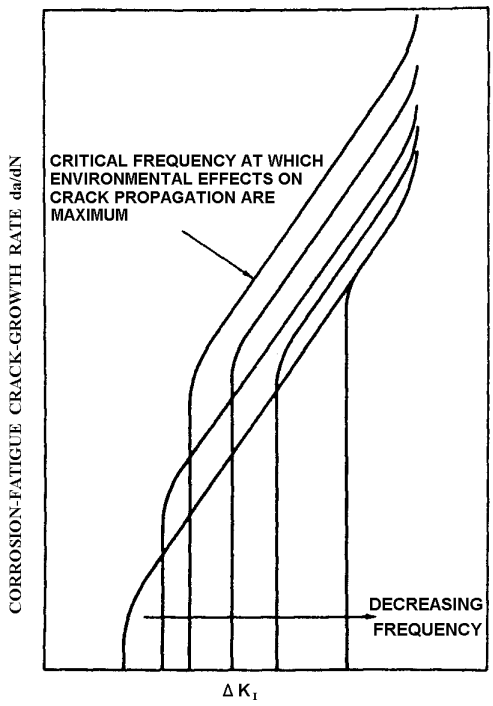

Fig. 2 Chart of idealized corrosion-fatigue characteristics being a function of cyclic-load frequency

Corrosion-fatigue-crack-propagation behaviour is a very complex phenomenon. This behaviour is strongly dependent on many variables, including frequency, waveform, and stress ratio. Tests at low frequencies are arduous, time consuming, and very expensive for region II behaviour and are precluditive for the threshold behaviour. Consequently, a clear understanding of the corrosion-fatigue behaviour in the various regions does not exist at the present time. However, based on the available data, a simplified schematic characterization of this behaviour may be accomplishable.

In an air environment, the fatigue ΔK_I threshold, ΔK_{th}, in various steels tested at a stress ratio, R, of 0.1 is independent of cyclic-load frequency and is equal to about 6.162 MPa √m. Because inimical environmental effects decrease with increased cyclic-load frequency, the corrosion-fatigue ΔK_{th} at very high cyclic-load frequencies would have a value close to that of fatigue in air. A K_{Iscc} test can be considered a corrosion-fatigue test at extremely low cyclic-load frequency. In such tests, the rate of crack growth at a stress-intensity-factor fluctuation that is slightly lower K_{Iscc} is, by definition, equal to zero. Consequently, at extremely low cyclic-load frequencies, ΔK_{th} should be equal to $K_{Iscc.}$ Hence, the value of the environmental ΔK_{th} at intermediate cyclic-load frequencies must be greater than 6.162 MPa√m and less than the value of K_{Iscc} for the environment-material system consider. The test results show that, at 12 cpm, the environmental ΔK_{th} for A 514 steels (analogous to Steel Grade 16224 in the Czech denomination) in 3 percent solution of sodium chloride in distilled water was equal to about 12.33 MPa√m. Based on the preceding observations, a schematic representation of the corrosion-fatigue behaviour of steels subjected to different cyclic-load frequencies has been plotted (Fig. 2). This figure is an oversimplification of a very complex phenomenon.

Although significant proficiencies have been made in understanding the corrosion-fatigue behaviour for some metal-environment systems, more is needed to improve the procedures for material choice analysis of engineering structures that are subjected to cyclic loads in aggressive environments.

SIMULATING CORROSION FATIGUE PROCESSES

Crack growth rate in conventional corrosion-fatigue analyses assessed fatigue damage by the addition of the metal dissolving rate and the fatigue crack growth rate in air. Superposition, but still, would imply that any dominant barrier to corrosion fatigue crack growth would remain the same as that in air, which is not the case recorded in experiments. Within this framework it is also difficult to incorporate fully the processes of pit initiation and growth (an important phase in corrosion fatigue) and to characterize the effect of an aggressive environment on the Stage I-to-Stage II transition, which is considered to be the major element of the fatigue resistance in air of a polycrystalline metal [3].

In this paper, contemplation is presented to pit initiation and growth, to the transition from Stage I – to- Stage II, and to the modification of the strain hardening law to conform to a parabolic law. These new progresses, when incorporated into the N-R model, improve our command of short fatigue crack growth characteristics and makes more accurate and satisfactory predictions of crack growth and fatigue life of a steel subject to an aggressive environment possible.

In corrosion fatigue, the contribution of an early crack growth phase as witnessed in a non-aggressive environment is of little consequence because the presence of the aggressive environment greatly reduces the in-air fatigue barrier strength and significantly accelerates the early crack initiation and growth processes due to the interaction of pitting and crack growth processes. It is this interaction that includes the major difference between the in-air fatigue and the corrosion fatigue lifetime of a material.

In a corrosive environment, pits are usually found at the origin of fracture surfaces of industrial machinery parts as well as on laboratory specimens. This implies that development of a pit starts fatigue crack propagation. Therefore, the quantitative evaluation of pitting is very important in the prediction of corrosion-fatigue behaviour. Experimental evidence has shown that the diameter of the major pit which eventually created a dominant fatigue crack, increased as a function of time (t), i.e. $t^{1/3}$. This observation can be explained using a simple dissolution law. For example, assuming a hemispherical pit of radius (r) and constant dissolution rate (A), the pit volume increases in proportion with time:

$$\frac{2}{3}\pi r^3 = At \tag{1}$$

or

$$2r = Bt^{1/3} \tag{2}$$

But, the incubation time for the formation of a major pit t_0, and the original size of the pit should be taken into account. Accordingly a corrosion pit growth law can be written down in the form:

$$2r - 2r_0 = B(t - t_0)^{1/3} \tag{3}$$

where $2r_0$ is the initial pit diameter corresponding to an inclusion or other defect, while t_0 is the incubation period.

The incubation time for the formation of a major pit and the constant B are given for a special high strength steel, they read

$$\ln t_0 = 16.71 - 0.0293\tau \tag{4}$$

and

$$(1/B)^3 = 0.191 - 0.00019\tau \tag{5}$$

where τ is the amplitude applied of shear stress cyclically. Experimental observations showed that the critical pit depth, denoted by H_c, at the transition from pit to crack, depended on the cyclic stress amplitude. For example at higher stress levels, the transition occurred at relatively small pits. Table 1 shows the variation of critical pit size in relation to the applied shear stress amplitude. The critical pit size, being a function of the applied stress amplitude, can be expressed by the following relation:

$$\log_{10} H_c = 1.921 - 0.00147\tau \tag{6}$$

for the material and environmental conditions used in our experiments. The values of t_0, H_0, H_c and $(1/B)^3$ for each stress level are listed in Table 2. The value of H_0 corresponds to the initial depth of the pit.

Substituting Eqs (4), (5) and (6) into Eq. (3) the major corrosion pit size as a function of applied stress amplitude is obtained, as is the pit growth rate. When a pit reaches the critical size, H_c, a crack develops from the pit and the time t for the pit to achieve this critical size, is taken as the pit development time. Because the number of loading cycles is proportional to time, i.e. $t=N/f$, where f is the cyclic frequency, then from Eq. (3) it results:

$$2r - 2r_0 = B[(N - N_0)/f]^{1/3} \tag{7}$$

Table 1. Values of parameters for modelling leading pit growth in Eqs (4), (5) and (6). The state, 0.06M NaCl solution at pH=6.5, and frequency = 5 Hz

Specimen	τ MPa	t_0 Seconds	$(1/B)^3$	H_c μm	K_{t0}
1	112	679760	0.16937	57	2.05
2	207.4	43610	0.15113	41	2.05
3	216.5	33502	0.14938	40	2.05
4	251.8	11987	0.14256	36	2.05
5	273.5	6395	0.13839	33	2.05
6	304.6	2597	0.13240	30	1.75
7	305.9	2492	0.13213	30	1.75
8	306.5	2449	0.13201	30	1.75
9	364.3	465	0.12099	24	1.5
10	371.1	373	0.11953	24	1.5
11	462.9	200	0.10231	18	1.5

Table 2. The final major pit length, H_c, the initial pit size, H_0, the dissolution rate, B, and the incubation time, t_0, obtained from tests at different stress amplitudes

Specimen	τ μm	t_0 (seconds)	$(1/B)^3$	H_c μm	H_0 μm
1	112			60	
2	207.4	55010	0.1251	35	0
8	306.5	1904	0.1186	32	0
9	364.3	865	0.1991	27	9
10	371.1	225	0.1318	25	12
11	462.9	25	0.05139	16	3

replacing $2r$ by H, and $2r_0$ by H_0, one has the pit growth rate:

$$\frac{\mathrm{d}H}{\mathrm{d}N} = \frac{B^3}{3f}\left(\frac{1}{H - H_0}\right)^2 \tag{8}$$

When the average growth rate is used to describe pit propagation behaviour, the expression can be performed as follows:

$$\overline{\left(\frac{\mathrm{d}H}{\mathrm{d}N}\right)} = \frac{1}{(t_2 - t_1)}\int_{t_1}^{t_2}\frac{\mathrm{d}H}{\mathrm{d}N}\mathrm{d}t = \frac{1}{(t_2 - t_1)}\int_{t_1}^{t_2}\frac{\mathrm{d}H}{\mathrm{d}N}\frac{\mathrm{d}N}{f} = \frac{1}{f(t_2 - t_1)}\int_{t_1}^{t_2}\mathrm{d}H = \frac{H_2 - H_1}{N_2 - N_1}$$

$$= \frac{B^3}{3f}\left[\frac{1}{(H_2 - H_0)^2 + (H_2 - H_0)(H_1 - H_0) + (H_1 - H_0)^2}\right] \tag{9}$$

where t_1 is the time for the pit to grow from H_0 to H_1 and t_2 is the time for the pit to grow from H_0 to H_2.

From Eq. (8) the number of cycles for pit growth may be derived in the form:

$$N_{\mathrm{pit}} = f\left(t_0 + (H_c - H_0)^3\left(\frac{1}{B}\right)^3\right) \tag{10}$$

Whenever the shear stress, resolved on the slip plane and in the slip direction, is greater than the initial internal friction stress τ_0, dislocation slip is generated. This is a microstructural process that usually takes place in the larger and optimally oriented grains. Due to this localization of strain cracks are formed and grow along the slip bands [4]. Slip is arrested on reaching the microstructural barrier which, in the present case, is the grain boundary, and the dislocations heap up against the barrier along the slip band giving rise to a stress concentration ahead of the plastic zone.

The critical condition for the plastic zone to overcome the barrier will be achieved when the crack length is such that n reaches the value of $n_{\mathrm{i}}^{\mathrm{c}}$, satisfying the critical equilibrium condition. Once the critical equation is satisfied the plastic zone extends to encompass the whole of the next grain and consequently $n_{\mathrm{i}}^{\mathrm{c}}$ jumps concurrently to:

$$n_{\mathrm{i+2}}^{\mathrm{s}} = n_{\mathrm{i}}^{\mathrm{c}}\frac{i}{i+2} \tag{11}$$

The crack growth rate is assumed to be proportional to the displacement between the two crack surfaces ahead of the crack tip, which in turn is equal to the number of dislocations entering the plastic zone, multiplied by the Burgers vector. Performing the integration, the plastic displacement ϕ can be related in the following manner:

$$\phi_i = \frac{2b}{\pi^2 A}\tau_f c_i\left[n_i \ln\left(\frac{1}{n_i}\right) + \sqrt{1 - n_i^2}\left(\frac{\pi}{2}\frac{\tau}{\tau_f} - \cos^{-1} n_i\right)\right] \tag{12}$$

Accordingly, the propagation rate of the crack equals:

$$\frac{\mathrm{d}a_i}{\mathrm{d}N} = \alpha(\phi_i)^m \tag{13}$$

where α and m are the material and environmental-dependent parameters. The factor α is interpreted as the fraction of dislocations on the slip band which participates in the process of crack extension. The dislocation movement is also expected to be affected by the presence of the aggressive environment, leading to different values of α and m as compared with "in-air" fatigue behaviour.

The above propagation law indicates that fatigue crack growth is an accumulation process of local plasticity. A similar law has been used by other researchers. When m=1, it becomes identical to the widely used laws of Elastic-Plastic Fracture Mechanics (EPFM).

Once a fatigue crack has been initiated, the value of n_i is low, just above zero, and therefore the crack growth rate is high, according to Eqs (12) and (13). As the crack grows, and with the plastic zone obstructed by the grain boundary, the value of n_i increases to such an extent that one of two possibilities may occur: if equality in the critical condition is not satisfied, the crack reaches the grain boundary at which point n_i=1, ϕ=0, and the crack will be arrested. Alternatively the critical condition is satisfied for a given $n_i = n_{\mathrm{i}}^{\mathrm{c}}$ and consequently the stress concentration ahead of the plastic zone or within the barrier zone will attain the critical value to activate a slip band in the next grain, at which point the value of c_i=iD/2 jumps to its new value of c_{i+2}=(i+2)D/2 and, accordingly, the parameter $n_i = n_{\mathrm{i}}^{\mathrm{c}}$ jumps to the new value $n_{\mathrm{i+2}}^{\mathrm{s}}$ which is evaluated by Eq. (11). Since ϕ is a function of n_i and τ, for a given value of i, the growth rate of the crack is thereby determined.

The crack growth mechanism illustrated here explains satisfactorily the oscillation pattern between low and high rates of short crack growth. When the crack becomes longer, the variation in n_i is much reduced (refer to Eq. (11)), and the growth rate gradually and steadily increases until it tends towards the EPFM regime previously described by Tomkins. The constancy in n after the fusion zone between MFM and EPFM reflects the preservation of geometrical analogy in the long crack regime.

From Eq. (12) it follows

$$\lim_{n_i^c \to 1} \phi_i = 0 \tag{14}$$

The growth law described by Eq. (13) indicates that the growth rate will tend to zero when the microstructure barrier is too strong for the applied load ($n_i^c \to 1$). This is the case of applied stresses below the fatigue limit level. Conversely, for propagating cracks, integration of Eq. (13), with limits for crack length from the initiation size a_0 to the failure size a_f, yields the crack propagation life in the form:

$$N = \int_{a_0}^{a_f} \frac{\mathrm{d}a_i}{\alpha(\phi_i)^m} = \sum_{i=1}^{i^{in}} \int_{a_i^s}^{a_i^c} \frac{\mathrm{d}a_i}{\alpha(\phi_i)^m} \tag{15}$$

In Eq. (15) $a_1^s = a_0$, while a_i^c is determined by the critical condition and a_i^s by Eq. (11). The term i^{in} relates to the actual condition of instability which occurs at the earliest of the three possibilities mentioned previously.

To perform the integration, bearing in mind that the plastic zone is blocked at a particular value of c_i, and n_i changes from n_i^s to n_i^c, subsequently the inserting $\mathrm{d}a_i = c_i \mathrm{d}n_i$ into Eq. (15) prompts to:

$$N = \sum_{i=1}^{i^{in}} \int_{n_i^s}^{n_i^c} \frac{c_i \mathrm{d}n_i}{\alpha \left\{ \frac{2b}{\pi^2 A} \tau_f c_i \left[n_i \ln\left(\frac{1}{n_i}\right) + \sqrt{1-n_i^2}\left(\frac{\pi}{2}\frac{\tau}{\tau_f} - \cos^{-1} n_i \right) \right] \right\}^m}$$

$$= \frac{1}{\alpha} \sum_{i=1}^{i^{in}} \left(\frac{\pi}{4\kappa} \right)^m \left(\frac{iD}{2} \right)^{1-m} \int_{n_i^s}^{n_i^c} \left\{ \frac{\tau_f}{G} \left[n_i \ln\left(\frac{1}{n_i}\right) + \sqrt{1-n_i^2}\left(\frac{2}{\pi}\frac{\tau}{\tau_f} - \cos^{-1} n_i \right) \right] \right\}^{-m} \mathrm{d}n_i \tag{16}$$

Indicating

$$J_i = \int_{n_i^s}^{n_i^c} \left\{ \frac{\tau_f}{G} \left[n_i \ln\left(\frac{1}{n_i}\right) + \sqrt{1-n_i^2}\left(\frac{2}{\pi}\frac{\tau}{\tau_f} - \cos^{-1} n_i \right) \right] \right\}^{-m} \mathrm{d}n_i \tag{17}$$

$$\Delta_i = \left(\frac{\pi}{4\kappa} \right)^m \left(\frac{iD}{2} \right)^{1-m} J_i \tag{18}$$

next

$$N = \frac{1}{\alpha} \sum_{i=1}^{i^{in}} \left(\frac{\pi}{4\kappa} \right)^m \left(\frac{iD}{2} \right)^{1-m} J_i = \frac{1}{\alpha} \sum_{i=1}^{i^{in}} \Delta_i \tag{19}$$

The theoretical determination of the material and environment-dependent parameters α and m needs a thorough knowledge of dislocation storage, reversibility and annihilation in order to calculate the fraction of dislocations actually involved in crack extension. In the present aggressive environment, the combined action of dissolution and hydrogen embrittlement will affect the dislocation movement, and hence affect α and m. Therefore the theoretical determination of α and m are rather difficult at the present stage. It follows that an empirical determination of these factors by best-fitting of the experimental results is necessary.

A correlation of fatigue lifetimes versus stress amplitudes between the experimental results and the theoretical predictions was performed to derive α and m via the least square method for each group of specimens tested in laboratory air and those tested in 0.6M NaCl solution. After α and m have been obtained, a comparison between predicted growth rate with experimental results was carried out using Eq. (13).

Bearing in mind that the development and propagation of pits also contribute to the total failure lifetime, Eq. (19) only gives the crack propagation time, hereafter denoted as N_{crack}. The contribution due to pitting is given by Eq. (10) and in this way the total corrosion fatigue failure life can be derived by summing up the two parts, that is

$$N_T = N_{pit} + N_{\text{crack}} = f\left(t_0 + \left(h_c - h_0\right)^3 \left(\frac{1}{B}\right)^3 \right) + \frac{1}{\alpha} \sum_{i=1}^{i^{in}} \Delta_i \tag{20}$$

This analysis is applied to the high strength spring steel (see Table 3).

Table 3. Fatigue life predictions using the modified N-R model (Eqs (13) and (20) with m=1.9 and α=7514) together with experimental results for a 0.6M NaCl solution, pH=6.5, frequency = 5 Hz, at room temperature

Specimen	τ MPa	Number of cycles			
		Predicted			Experiment
		Pitting	Cracking	Total	
1	112	3555631	3481428	7037059	6500000
2	207.4	270130	627289	897419	870500
3	216.5	215312	550731	766043	795000
4	251.8	93191	352414	445605	553000
5	273.5	56841	284636	341477	310500
6	304.6	30854	200373	231227	259500
7	305.9	30297	197695	227992	192000
8	306.5	30066	196272	226338	205000
9	364.3	10687	118912	129599	174320
10	371.1	10127	110788	120915	132100
11	462.9	3483	52120	55603	73800

CONCLUSION

It is manifested that the model yields a good predictive method for fatigue crack growth characteristics and final failure. The good agreement confirms the fundamental physical facts that short fatigue crack growth is influenced by microstructural inhomogeneities and local impedance and that such behaviour cannot be represented by a single-value function, for instance the LEFM stress intensity factor. Instead crack growth characteristics is of a crystallographs and microstructure – sensitive nature. Based on a displacement representation of short cracks, Navarro-de los Rios model gives a useful basis on which to study the behaviour of microstructure – sensitive fatigue cracks.

A lower fatigue limit stands for that the microstructural obstacles are conquered much more promptly and this demonstrates that the crack tip does not need to be redeployed close to the barrier (a lower n_i^c) value in order to come over the barrier restriction. The influences of enhanced crack tip plasticity and crack dissolving are shown in the altered values of α and m in Eq. (13). Dissolution increases the number of displacements that, in the course of the opposite part of the fatigue cycle, enter the cracks to produce the growth step. The combination of all these factors signifies that a fatigue crack will grow at a higher rate in a corrosive environment in comparison to a neutral milieu.

REFERENCES

1. De los Rios, E.R., Wu, X.D. and Miller, K.J., "Micro-Mechanics Model of Corrosion-Fatigue Crack Growth in Steels", *Fatigue Fract Engng Mater Struct*, Vol. 19, No. 11, 1996, pp. 1383-1400.
2. Suresh, S., *Fatigue of Materials*, Cambridge University Press, 1992.
3. Miller, K.J., "Materials Science Perspective of Metal Fatigue Resistance", *Mater Sci Technol*, Vol. 9, 1993, pp. 453-462.
4. De los Rios, E.R., Xin, X.J. and Navarro, A., "Modelling Microstructurally – Sensitive Fatigue Short Crack Growth", *Proc R Soc Load*, Vol. 447, 1994, pp. 111-134.